

Site-specific imaging and spectral classification of subsurface targets

Arnold D. Kim and Chrysoula Tsogka

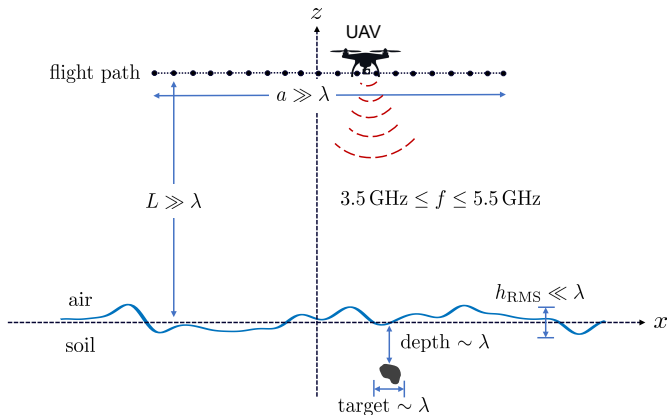
Department of Applied Mathematics
University of California, Merced

Supported by AFOSR (FA9550-24-1-0191)



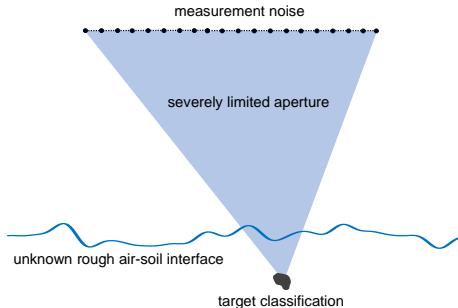
Motivation

We are studying unmanned aerial vehicle (UAV)-based ground penetrating synthetic aperture radar (SAR) for the buried landmine problem and related applications.



Challenges

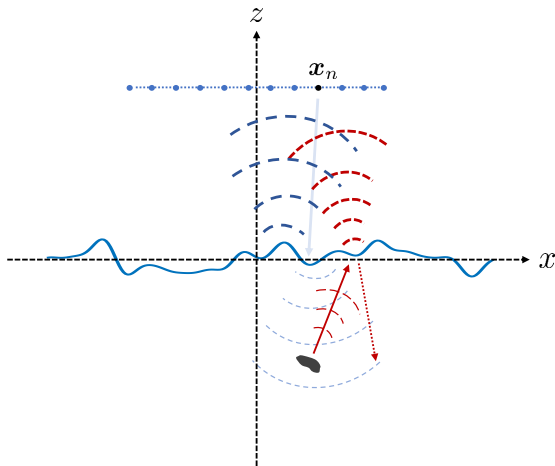
We restrict our attention to the following challenges for this subsurface imaging problem.



As we make progress, we plan to consider more, *e.g.* timing noise, clutter, unknown ground permittivity, etc.

Measurements

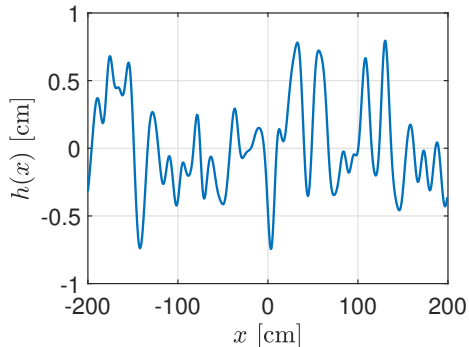
- ▶ Measurements are stored as the matrix $D \in \mathbb{C}^{M \times N}$.
- ▶ d_{mn} = measurement at frequency f_m at spatial location x_n on the flight path.
- ▶ Measurements contain ground bounce signals and scattered signals by the target.



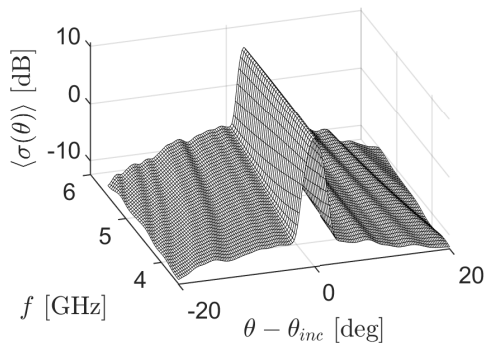
Ground bounce signals

Measurements are dominated by multiple scattering by the rough air-soil interface.

realization of rough surface



bistatic cross-section (100 realizations)



RMS height 0.4 cm and correlation length 8 cm.

Two-step imaging method

1. Principal component analysis (PCA) for ground bounce removal

$$D = U\Sigma V^H, \quad \tilde{D}_p = D - \sum_{j=1}^p \sigma_j \mathbf{u}_j \mathbf{v}_j^H.$$

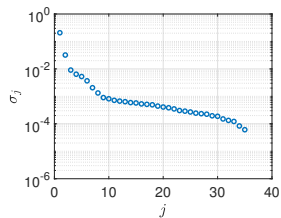
2. Kirchhoff migration (KM) for identifying and locating targets

$$I^{\text{KM}}(\mathbf{y}) = \sum_{m=1}^M \sum_{n=1}^N \tilde{d}_{mn} a_{mn}^*(\mathbf{y}), \quad a_{mn}(\boldsymbol{\rho}, \zeta) = e^{i2k_m(L + \sqrt{\epsilon_r}|\zeta|)} e^{ik_m|\mathbf{x}_n - \boldsymbol{\rho}|^2/L^2}.$$

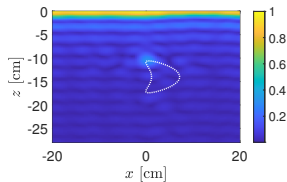
(illuminations $a_{mn}(\mathbf{y})$ are for a flat air-soil interface using the Fresnel approximation)

Imaging results

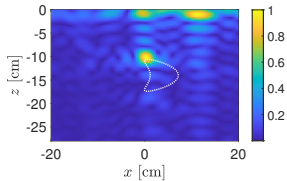
singular values



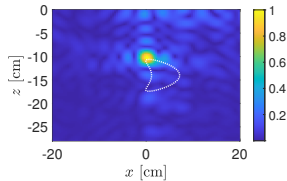
KM using D



KM using \tilde{D}_1



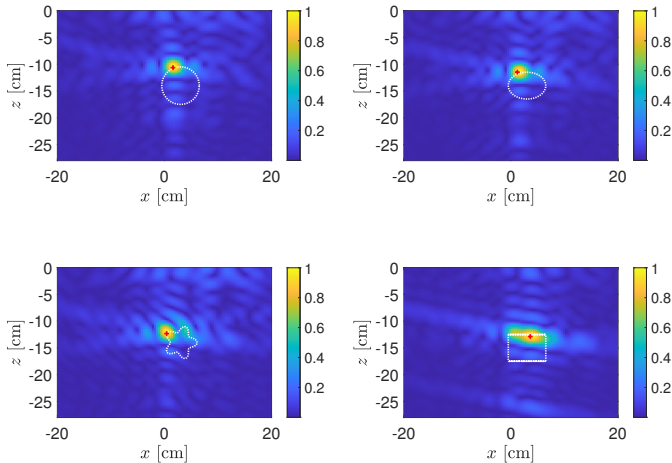
KM using \tilde{D}_2



Soil: $\epsilon_r = 9$, Target: $\epsilon_r = 2.3$.

Imaging for different target shapes

All targets have $\epsilon_r = 2.3$ and are comparable in size to the central wavelength.

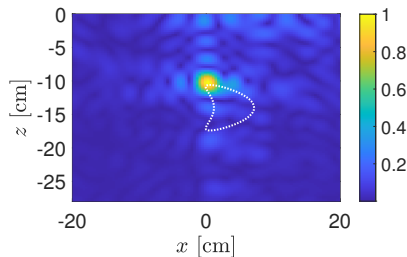


Inherent limitations in measurements

Scattering by a particle in the far-field:

$$u_s(R\hat{\boldsymbol{o}}) \sim U_\infty(\hat{\boldsymbol{o}}, \hat{\boldsymbol{i}}; k) \frac{e^{ikR}}{R}, \quad R \rightarrow \infty.$$

- Monostatic SAR: $\hat{\boldsymbol{o}} = -\hat{\boldsymbol{i}}$
- Flight path: $\hat{\boldsymbol{i}}$ subtends a relatively small range of directions.



Because of the inherent space/angle limitations in measurements, images only concentrate about a representative point for the target.

These inherent limitations suggest a simplified model for measurements may be useful.

Assumption 1: First-order target-interface interactions

We model measurements by only considering first-order interactions between the target and the air-soil interface.

absolute difference (\log_{10})

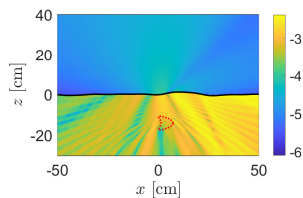


image using full data

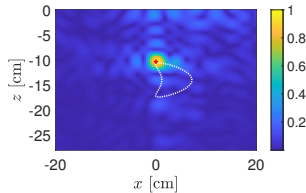
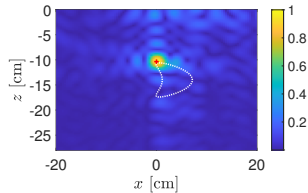


image using approximation



Assumption 2: Target scattering below a flat air-soil interface

The target depth below the air-soil interface is much smaller than the height of the UAV from it.

The shower curtain effect suggests that target scattering transmitted across air-soil interface does not depend strongly on its roughness.

absolute difference (\log_{10} -scale)

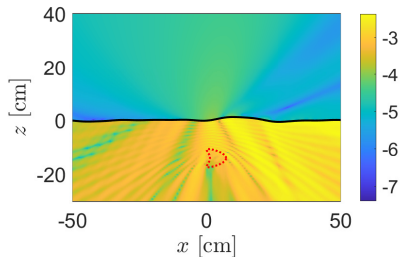
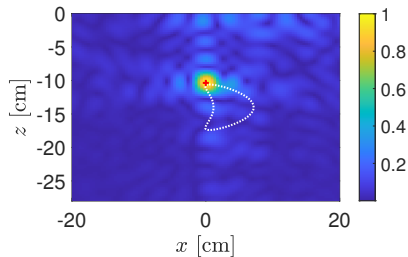


image using approximation



Assumption 3: Point target model

image using full data

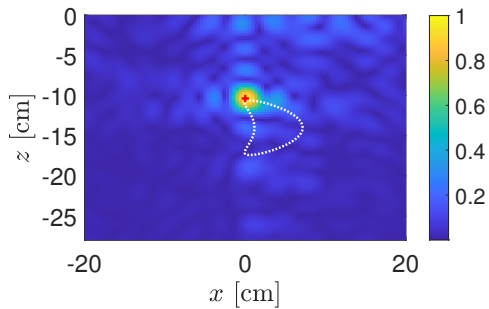
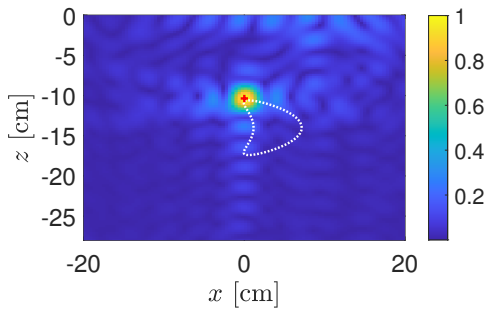


image using point target model



Modeling measurements

The results from these assumptions suggest the following model for ground penetrating SAR measurements:

$$D \approx D^{\text{model}} = R^{\text{rough}} + \varrho S^{\text{flat}}(\mathbf{r}_0),$$

with \mathbf{r}_0 denoting the location of the point target with reflectivity ϱ .

We can use this model to interpret the two-step imaging method as follows.

$$\tilde{D}_p \approx \varrho S^{\text{flat}}(\mathbf{r}_0) + E, \quad E = R^{\text{rough}} - \sum_{j=1}^p \sigma_j \mathbf{u}_j \mathbf{v}_j^H.$$

E acts as additive noise for KM.

Frequency dependent reflectivity

Extending our measurement model to include a frequency-dependent reflectivity leads to

$$D^{\text{model}} = R^{\text{rough}} + \text{diag}(\varrho_1, \dots, \varrho_M) S^{\text{flat}}(\mathbf{r}_0).$$

For a dispersive point target, the radar cross-section (RCS) is

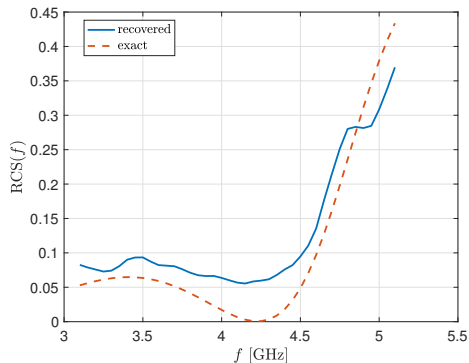
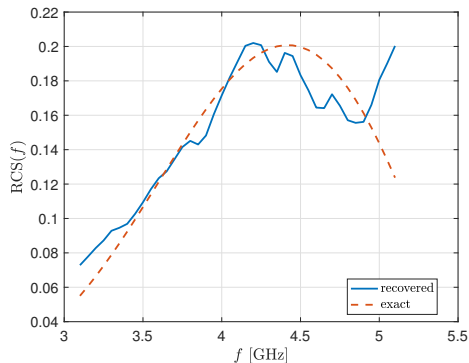
$$\text{RCS}(f) = 4\pi |\varrho(f)|^2.$$

Using the estimate $\hat{\mathbf{r}}_0$ we obtain from the KM image, we compute

$$\text{RCS}(f_m) \approx 4\pi \left(\frac{1}{N} \sum_{n=1}^N \frac{|\tilde{d}_{mn} a_{mn}^*(\hat{\mathbf{r}}_0)|}{|a_{mn}(\hat{\mathbf{r}}_0)|^2} \right)^2.$$

Recovery of the RCS

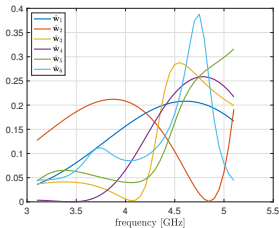
Because recovery of the RCS has scaling errors and spurious oscillations both due to modeling errors, we smooth and normalize those results.



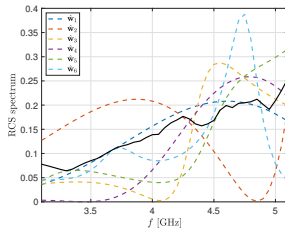
Spectral classification

Let $\hat{\mathbf{v}}$ denote the smoothed and normalized recovered RCS spectrum and \mathbf{W} a matrix whose columns contain a library of classes.

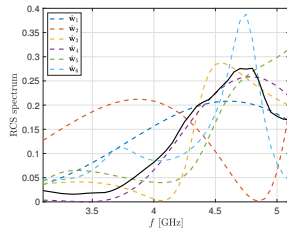
library



classified to $\hat{\mathbf{w}}_1$



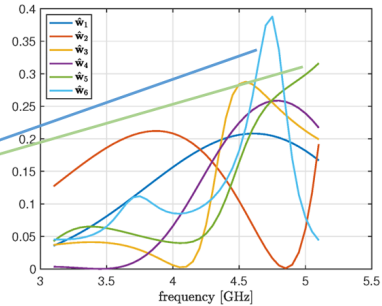
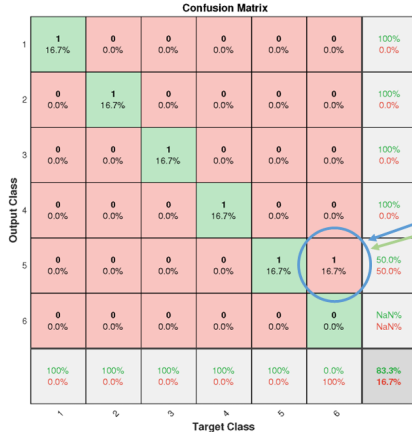
classified to $\hat{\mathbf{w}}_4$



We classify by computing $\mathbf{c} = \mathbf{W}^H \hat{\mathbf{v}}$ and find which entry of \mathbf{c} is largest.

Spectral classification results

We performed a Monte Carlo simulation with 36 different targets parameterized by size and relative permittivity.



Summary

- ▶ Simplified model for ground penetrating SAR measurements
(manuscript is currently under review)
- ▶ Spectral classification of dispersive targets
(published in IEEE Geoscience and Remote Sensing Letters)
- ▶ Theoretical frameworks
(in progress with graduate student Joseph Simpson and collaborator Pedro González-Rodríguez)